

Transfer vs. Breakup in the interaction of the ^7Be Radioactive Ion Beam with a ^{58}Ni target at Coulomb barrier energies

M. Mazzocco^{1,2}, D. Torresi^{1,2}, L. Acosta³, A. Boiano⁴, C. Boiano⁵, N. Fierro¹, T. Glodariu⁶, A. Guglielmetti^{5,7}, N. Keeley⁸, M. La Commara^{4,9}, I. Martel³, C. Mazzocchi^{5,7}, P. Molini^{1,2}, A. Pakou¹⁰, C. Parascandolo^{1,2}, V.V. Parkar³, N. Patronis¹⁰, D. Pierroutsakou⁴, M. Romoli⁴, K. Rusek¹¹, A.M. Sanchez-Benitez³, M. Sandoli^{4,9}, C. Signorini^{1,2}, R. Silvestri^{4,9}, F. Soramel^{1,2}, E. Stiliaris¹², E. Strano^{1,2}, L. Stroe⁶, K. Zerva¹⁰

¹Dipartimento di Fisica e Astronomia, Università di Padova, Via F. Marzolo 8, I-35131 Padova, Italy

²INFN-Sezione di Padova, Via F. Marzolo 8, I-35131 Padova, Italy

³Departamento de Fisica Aplicada, Universidad de Huelva, E-21071 Huelva, Spain

⁴INFN-Sezione di Napoli, Via Cinthia, I-80126 Napoli, Italy

⁵INFN-Sezione di Milano, Via Celoria 16, I-20133 Milano, Italy

⁶NIPNE, 407 Atomistilor Street, 077125 Magurele, Romania

⁷Dipartimento di Fisica, Università di Milano, Via Celoria 16, I-20133 Milano, Italy

⁸Department of Nuclear Reactions, Institute for Nuclear Studies, ul. Hoza 69, 00-681 Warsaw, Poland

⁹Dipartimento di Scienze Fisiche, Università di Napoli, Via Cinthia, I-80126 Napoli, Italy

¹⁰Department of Physics and HINP, The University of Ioannina, GR-45110 Ioannina, Greece

¹¹Heavy Ion Laboratory, University of Warsaw, ul. Pasteura 5a, 02-093 Warsaw, Poland

¹²Department of Physics, University of Athens, Athens, Greece

Abstract. We measured for the first time ^7Be elastically scattered nuclei as well as $^{3,4}\text{He}$ reaction products from a ^{58}Ni target at 22.3 MeV beam energy. The data were analyzed within the optical model formalism to extract the total reaction cross section. Extensive kinematical, Distorted Wave Born Approximation (DWBA) and Continuum Discretized Coupled Channel (CDCC) calculations were performed to investigate the $^{3,4}\text{He}$ originating mechanisms and the interplay between different reaction channels.

1 Introduction

The reaction dynamics induced by weakly-bound Radioactive Ion Beams (RIBs) at near-barrier energies has attracted the interest of the Nuclear Physics community for at least 20 years. Several review articles have been recently written on this topic (see for example [1] and references therein).

In the present case we studied the interaction of the ^7Be RIB with a ^{58}Ni target at two energies around the Coulomb barrier. ^7Be was chosen since it has a very small particle emission threshold ($S_\alpha = 1.586$ MeV) and since the majority of direct processes gives rise to either ^3He or ^4He stable ions (with similar energy domains) in the reaction output channels. This feature simplifies the experimental setup and avoids typical problems related to the low-efficiency detection of neutrons (as in $^{6,8}\text{He}$ -, $^{9,11}\text{Li}$ - and $^{9,11}\text{Be}$ -reaction studies), the emission of radioactive or loosely-bound nuclei (as in the case of reactions involving $^{6,7}\text{Li}$ or ^8B) or the detection of projectile fragments with completely different mass ranges, and in turn energy domains, (as for ^{17}F breaking up into $^{16}\text{O}+p$).

2 Experiment

The experiment was performed at the INFN-Laboratori Nazionali di Legnaro (LNL), where the ^7Be beam was delivered by the facility EXOTIC [2-4], now fully operational for the in-flight production of light weakly-bound RIBs. The ^7Be secondary beam was produced via the two-body reaction $p(^7\text{Li}, ^7\text{Be})n$ induced by a 34.2 MeV ^7Li primary beam, delivered by the LNL-XTU Tandem accelerator, impinging on H_2 gas target. The primary beam intensity was about 100 pA, the H_2 gas pressure was 1 bar and the target station was operated at liquid nitrogen temperature (~ 90 K), for a corresponding target thickness of 1.35 mg/cm^2 . The ^7Be secondary beam had an intensity of $2\text{-}3 \cdot 10^5$ pps and was nearly 100 % pure, as it can be seen in Fig. 2 of Ref. [5]. The outgoing ^7Be energy was 22.3 ± 0.4 MeV. This energy value is about 1 MeV lower than that originally quoted in Refs. [1,5] due to careful recheck of the energy calibration of the beam monitor detectors.

Charged reaction products were detected by means of the detector array DINEX [6]. For the present experiment we used 8 silicon detectors arranged in 4 ΔE (42-48 μm) - E (1000 μm) telescopes. Each detector had an active area of 48.5 mm x 48.5 mm and was segmented into 16 x 16 strips, allowing a position resolution of $3 \times 3 \text{ mm}^2$. The telescopes were placed in a barrel configuration around the target position at a mean distance of 70-72 mm, ensuring an overall solid angle coverage of about 10% of 4π sr. The mean polar angles of the four telescopes were $\theta_{\text{lab}} = +57^\circ$ (T1), $+128^\circ$ (T2), -61.5° (T3) and -132° (T4). Finally, the ^{58}Ni target was 1 mg/cm^2 thick.

3 Quasi-Elastic Scattering

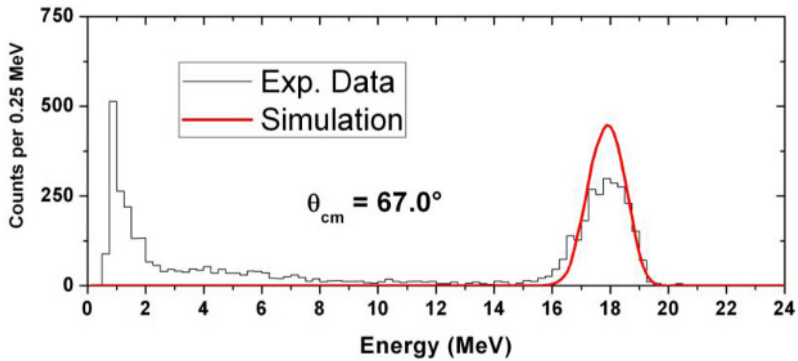


Figure 1. Total energy spectrum for the system $^7\text{Be}+^{58}\text{Ni}$ at 22.3 MeV recorded by the vertical strip of telescope T1 located at $\theta_{\text{cm}} = +67.0^\circ$ (black histogram). The continuous (red) line represents the simulated energy spectrum for a pure elastic scattering process. See text for additional details.

The black histogram in Fig. 1 represents a typical total energy spectrum collected at the higher secondary beam energy by a vertical detector strip located at forward angles. The continuous (red) line is the result of a Monte-Carlo simulation for a pure elastic scattering process. The simulation takes into account the secondary beam energy resolution, the beam spot on target (FWHM about 8-9 mm), the energy loss into the target thickness prior and after the scattering process, the kinematics of the elastic scattering process, the geometry of the detector array and the detector energy resolution. The simulated data were normalized at very forward angles ($\theta_{\text{cm}} < 60^\circ$), where the elastic scattering angular differential cross section is described by the well-known Rutherford formula. The ratio between the integrals of the experimental and the simulated spectrum in the energy range of elastic scattering events essentially gives the ratio-to-Rutherford ($d\sigma/d\sigma_{\text{Ruth}}$) at the mean polar angle of the considered detector strip. Fig. 2 shows the elastic scattering angular distribution evaluated for the system $^7\text{Be} + ^{58}\text{Ni}$ at 22.3 MeV beam energy. Since the secondary beam energy resolution and the target thickness did not allow to separate inelastic excitations leading to the projectile ($Ex = 0.429$

MeV) and target ($E_x = 1.414$ MeV) excited states from pure elastic scattering events, the data plotted in Fig. 2 have to be considered quasi-elastic.

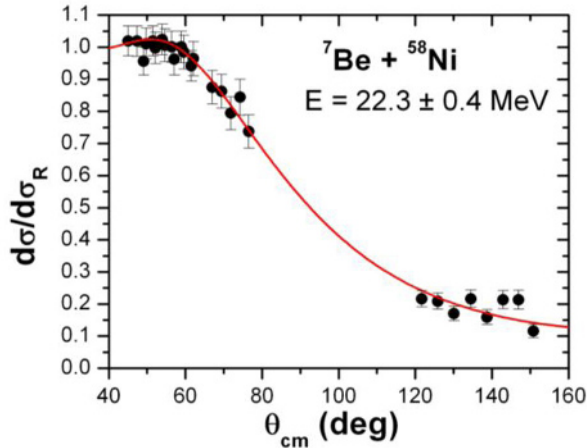


Figure 2. Quasi-elastic scattering angular distribution for the system ${}^7\text{Be} + {}^{58}\text{Ni}$ at 22.3 MeV. The continuous (red) line represents the optical model best-fit analysis of the collected data.

A preliminary analysis within the formalism of the optical model with the code FRESKO [7] gave a total reaction cross section of 561 ± 36 mb, in good agreement with the trend of the total reaction cross section data obtained by E.F. Aguilera and collaborators at lower beam energies [8].

4 ${}^{3,4}\text{He}$ Production Cross Sections

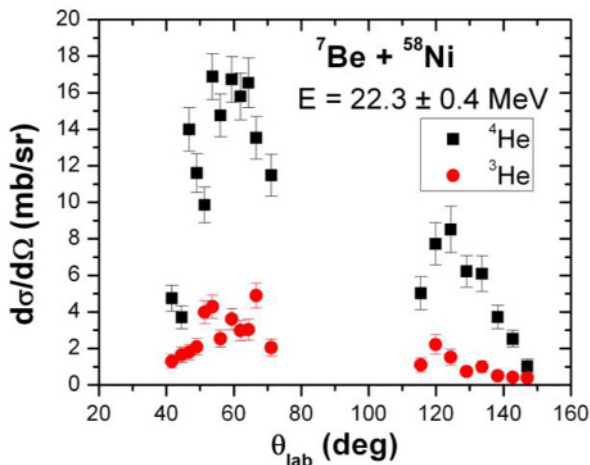


Figure 3. ${}^{3,4}\text{He}$ angular distributions measured for the reaction ${}^7\text{Be} + {}^{58}\text{Ni}$ at 22.3 MeV secondary beam energy.

Fig. 3 shows the angular distributions for ${}^{3,4}\text{He}$ reaction products measured for the system ${}^7\text{Be} + {}^{58}\text{Ni}$ at 22.3 MeV beam energy. We immediately realize that ${}^4\text{He}$ ions are about 5 times more abundant than ${}^3\text{He}$ nuclei. The angle-integrated cross sections for ${}^4\text{He}$ and ${}^3\text{He}$ sum up to ~ 160 mb and ~ 28 mb, respectively. This outcome indicates that the two helium isotopes should originate from different reaction mechanisms. Indeed, in case the main source of ${}^3\text{He}$ and ${}^4\text{He}$ were the exclusive breakup process ${}^7\text{Be} \rightarrow {}^3\text{He} + {}^4\text{He}$, we would have expected similar yields for the two isotopes. We therefore started to investigate the possible processes which may trigger the production of ${}^3\text{He}$ and ${}^4\text{He}$.

4.1 ^3He production

The interaction of ^7Be projectiles with a ^{58}Ni target can essentially produce ^3He ions by two main processes: (i) exclusive breakup: $^7\text{Be} \rightarrow ^3\text{He} + ^4\text{He}$ and (ii) ^4He -stripping: $^7\text{Be} + ^{58}\text{Ni} \rightarrow ^3\text{He} + ^{62}\text{Zn}$ ($Q_{\text{gg}} = +1.78$ MeV). The fact that we did not record any ^3He - ^4He coincidences (clear signature of exclusive breakup events) and the shape of the ^3He energy spectra collected at both forward and backward angles indicate the ^4He -stripping as the main responsible process for the ^3He production.

4.2 ^4He production

The situation is more colourful for the ^4He production since we have a larger variety of triggering reaction mechanisms: (i) exclusive breakup: $^7\text{Be} \rightarrow ^3\text{He} + ^4\text{He}$; (ii) ^3He -stripping: $^7\text{Be} + ^{58}\text{Ni} \rightarrow ^4\text{He} + ^{61}\text{Zn}$ ($Q_{\text{gg}} = +9.46$ MeV); (iii) n-stripping: $^7\text{Be} + ^{58}\text{Ni} \rightarrow ^6\text{Be} (= ^4\text{He} + \text{p} + \text{p}) + ^{59}\text{Ni}$ ($Q_{\text{gg}} = -1.68$ MeV); (iv) n-pickup: $^7\text{Be} + ^{58}\text{Ni} \rightarrow ^8\text{Be} (= ^4\text{He} + ^4\text{He}) + ^{57}\text{Ni}$ ($Q_{\text{gg}} = +6.68$ MeV) and (v) ^4He -evaporation after a compound nucleus reaction. Reaction mechanisms (i), (iii) and (iv) will produce at least a pair of charged particles in the reactions exit channel. Experimentally, we did not observe any ^4He - ^3He (breakup), ^4He -p (n-stripping) and ^4He - ^4He (n-pickup) coincidences. Within the geometrical efficiency of our detector array, we can set an upper limit (preliminary evaluation) of 3, 7 and 6 mb for the exclusive breakup, n-stripping and n-pickup process, respectively. Distorted Wave Born Approximation (DWBA) and Continuum Discretized Coupled Channel (CDCC) calculations performed with the code FRESKO indicate for these three processes the following cross sections: 9.3, 10.3 and 5.8 mb, respectively. We can see that there is a reasonably good agreement between experimental outcomes and theoretical predictions. Moreover, the shapes of the ^4He energy spectra collected both at forward and backward angles are rather compatible with those predicted for the ^3He -stripping transfer and for the fusion-evaporation process. The discussion about the limits imposed by our analysis to the cross sections of these two reaction mechanisms will be the subject of a forthcoming paper.

5 Summary

We measured for the first time the interaction of the ^7Be RIB with a ^{58}Ni target at 22.3 MeV. The optical model analysis of the quasi-elastic angular distribution provided the measurement of the total reaction cross section, which turned out to be in good agreement with the trend of the data collected at lower beam energies. We performed a quite sophisticated theoretical and kinematical analysis of the angular distributions for the $^{3,4}\text{He}$ reaction products. According to the preliminary results of our work, the origin of ^3He and ^4He is mainly attributed to transfer channels, namely ^4He -stripping and ^3He -stripping, respectively. A quite relevant contribution to the ^4He production cross section may also arise from fusion-evaporation reactions and this issue will deserve further investigations. This work was partially supported by the Italian M.I.U.R. within the project RBFR08P1W2_001 (FIRB 2008).

References

1. M. Mazzocco et al., *Acta Phys. Pol. B* **44**, 437 (2013)
2. F. Farinon et al., *Nucl. Instrum. Meth. B* **266**, 4097 (2008)
3. M. Mazzocco et al., *Nucl. Instrum. Meth. B* **266**, 4665 (2008)
4. M. Mazzocco et al., *Nucl. Instrum. Meth. B* doi:10.1016/j.nimb.2013.06.031 (in press)
5. M. Mazzocco et al., *Journal of Physics: Conf. Series* **420**, 012077 (2013)
6. A.M. Sanchez-Benitez et al., *J. Phys. G* **31**, S1953 (2005)
7. I.J. Thompson, *Comput. Phys. Rep.* **2**, 167 (1988).
8. E.F. Aguilera et al., *Phys. Rev. C* **79**, 021601 (2009)